observation of incomplete spin transitions in a number of the present examples probably results from effects such as grinding of the crystallites or the exact conditions used for synthesis and isolation. Hendrickson[13,14] has explained such effects in terms of some of the Fe^{III} Schiff-base molecules (i.e. a minority domain of particular spin-state) existing in a slightly different crystalline environment to the bulk of the molecules. This could result from crystal defects caused either by mechanical aggravation or more subtle effects such as the presence or absence of trace amounts of solvent molecules. Defects at the domain edge are then capable of influencing the spin transition. It seems to us, however, that it is difficult to adequately explain Mössbauer spectra of the type exhibited by complexes such as $[Fe(salen)(imd)_2]ClO_4$ using domain theory. Because the relaxation time of the high-spin state to the low-spin state is faster than the Mössbauer lifetime ($\sim 10^{-7}$ s), a ^{57}Fe nucleus "sees" an average spin state. In such a situation it is difficult to envisage how a minority domain could interact with a neighboring domain and trigger the spin transition. It is tempting to favor the Ising type random distribution model of König[33] and Gütlich,[32] especially above and below the transition temperature, where the percentage of molecules of the "second" spin state is very small in cases of complete spin transition and larger in incomplete transitions. At the actual crossover region complex electronic interactions are occurring. It is possible that the increase of the minority spin occurs in a much more systematic manner throughout the lattice than implied by the expression "random distribution".

Acknowledgment. We gratefully acknowledge the receipt of grants from the Australian Research Grants Scheme (K.S.M. and A.H.W.) and Monash University Special Research Grants (K. S.M.) in support of this work. We thank Dr. J. D. Cashion, Dr. J. R. Pilbrow, and G. Brain for help with Mössbauer and ESR spectral studies.

Supplementary Material Available: Tables SUP1-4 (non-hydrogen atom anisotropic thermal parameters for $[Fe(salen)(imd)_2]Y$, where Y = ClO_4^- (120 K, **1a**; 295 K, **1b**), BF_4^- (**2**), PF_6^- (**3**), respectively), Tables SUP5 and SUP6 (hydrogen atom parameters for **1a,b** and for **2** and **3**, respectively), Tables SUP7 and SUP8 (least-squares planes for salen ligands and imidazole rings, respectively), and Table SUP9 (microanalytical data) (16 pages); Table SUP10 (structure factors for **1a,b**, **2**, and **3**) (56 pages). Ordering information is given on any current masthead page.

Contribution from the Department of Chemistry, University of Michigan, Ann Arbor, Michigan 48109

Characterization of Mono- and Binuclear Manganese(II) Schiff Base Complexes with Metal-Disulfide Ligation

Dimitri P. Kessissoglou,[1] William M. Butler, and Vincent L. Pecoraro*

Received March 28, 1986

Both mononuclear and binuclear complexes of Mn^{2+} with the Schiff base disulfide ligand *N,N'*-[1,1'-dithiobis(phenylene)]bis(salicylideneaminato) (SALPS) have been synthesized and characterized by electrochemical, magnetic, spectral, and diffraction methods. SALPS acts as a pentadentate ligand using one disulfide sulfur atom and two oxygen and two nitrogen atoms to bind Mn^{2+} forming Mn(SALPS)solvent in donor solvents. $Mn(SALPS)CH_3OH{\cdot}CH_3OH$ crystallizes in the triclinic crystal system, space group $P\bar{1}$, with $Z = 2$, $a = 9.692$ (2) Å, $b = 11.195$ (4) Å, $c = 13.399$ (5) Å, $\alpha = 110.47$ (3)°, $\beta = 94.57$ (3)°, $\gamma = 98.95(3)$°, and $V = 1331.2$ (9) Å^3. The refinement converged with $R = 0.029$ and $R_w = 0.031$ based on 2984 reflections with $I > 3\sigma(I)$. $Mn(SALPS)CH_3OH$ describes a highly distorted octahedral complex with a Mn(II)-S bond length of 2.77 Å. Magnetic and EPR data support the assignment of the manganese oxidation state in this complex. In solvents such as acetonitrile, toluene and methylene chloride, the basic coordination environment is retained; however, solvent is displaced and a bis(μ-phenolato) dimer, $[Mn(SALPS)]_2$, is formed. $[Mn(SALPS)]_2{\cdot}2CH_3CN$ also crystallizes in the triclinic crystal system, space group $P\bar{1}$, with $Z = 2$, $a = 12.311$ (9) Å, $b = 14.818$ (6) Å, $c = 15.141$ (5) Å, $\alpha = 109.99$ (3)°, $\beta = 84.76$ (5)°, $\gamma = 103.33$ (5)°, and $V = 2525$ (3) Å^3. The refinement converged with $R = 0.040$ and $R_w = 0.038$ for 3596 reflections with $I > 3\sigma(I)$. X-ray structural analysis indicates that the manganese ions are separated by 3.30 Å. A complex EPR signal is observed for the dimer in toluene at 90 K, suggesting that the centers are weakly coupled. Analysis of variable-temperature magnetic susceptibility data (1.9-298 K) shows that the manganese ions are antiferromagnetically coupled with $J = -1.88$ (6) cm^{-1} and $g_{av} = 2.00$. Both the monomer and the dimer show completely irreversible cyclic voltammetric traces in DMF and methylene chloride.

Introduction

The synthesis and characterization of manganese coordination complexes are useful toward the understanding of the structure and reactivity of manganese sites in biological systems. Besides an apparent role as a metal ion cofactor in certain ATP utilizing reactions,[2] there are a number of essential functions for which manganoenzymes have been implicated. Among these are detoxification enzymes such as superoxide dismutase[3,4] and pseudocatalase,[5] which respectively use superoxide and hydrogen peroxide as substrates. A multinuclear manganese center has been proposed for the active site of the thylakoid-membrane-associated oxygen-evolving complex of photosystem II.[6-8] Recently, an enzyme that displays acid phosphatase activity has been isolated from sweet potatoes.[9] It is believed that this enzyme contains a Mn(III)-S bond.[10,11] This is a fascinating center since it requires the coexistence of a moderate oxidant, Mn(III), with a thiolate residue, a well-established reducing agent. Manganese(III) ethanedithiolate complexes have been characterized crystallographically;[12-14] however, in most cases Mn(III)-thiolates undergo

(1) Present address: Laboratory of Inorganic Chemistry, Aristotelian University of Thessaloniki, Thessaloniki, Greece.
(2) Weissiger, R. A.; Fridovich, I. *J. Biol. Chem.* **1973**, *248*, 3582.
(3) Stallings, W. C.; Pattridge, K. A.; Strong, R. K.; Ludwig, M. L. *J. Biol. Chem.* **1984**, *256*, 10664.
(4) Kono, Y.; Fridovich, I. *J. Biol. Chem.* **1983**, *258*, 13646.
(5) Beyre, W. F., Jr.; Fridovich, I. *Biochemistry* **1985**, *24*, 6460.
(6) Radmer, R.; Cheniae, G. *Primary Processes of Photosynthesis*; Barber, J., Ed.; Elsevier/North Holland Biomedical: Amsterdam, 1977, 305.
(7) Dismukes, G. C.; Siderer, Y. *Proc. Natl. Acad. Sci. U.S.A.* **1981**, *78*, 274.
(8) de Paula, J. C.; Brudvig, G. W. *J. Am. Chem. Soc.* **1985**, *107*, 2643.
(9) Suguira, Y.; Kawabe, H.; Tanaka, H. *J. Am. Chem. Soc.* **1980**, *102*, 6581.
(10) Suguira, Y.; Kawabe, H.; Tanaka, H.; Fujimoto, S.; Ohara, A. *J. Am. Chem. Soc.* **1981**, *103*, 963.
(11) Kawabe, H.; Sugiura, Y.; Terachi, M.; Tanaka, H. *Biochim. Biophys. Acta* **1984**, *784*, 81.
(12) Seela, J. L.; Huffman, J. C.; Christou, G. *J. Chem. Soc., Chem. Commun.* **1985**, 58.

0020-1669/87/1326-0495$01.50/0 © 1987 American Chemical Society

internal redox reactions, ultimately forming Mn(II) and disulfides.

As part of our studies on the bioinorganic chemistry of manganese we are investigating the coordination chemistry of Mn(II) and Mn(III) with sulfur ligands. We have been successful in isolating interesting ligand-centered oxidation products while attempting to prepare Mn(III) thiolates through controlled aerial oxidation of Mn(II) arylenethiolates. In this paper we report the synthesis and properties of the complexes formed by Mn(II) with the Schiff base disulfide ligand SALPS,[15] *N,N'*-[1,1'-dithiobis(phenylene)]bis(salicylideneaminato). We have isolated and characterized the monomeric material $Mn^{II}(SALPS)CH_3OH$ and its dimeric form $[Mn^{II}(SALPS)]_2$ by electrochemical, magnetic, spectroscopic, and X-ray diffraction methods.

Experimental Section

Preparation of Compounds. (a) [Mn(SALPS)CH_3OH]·CH_3OH. Method 1. A 2.16-mL (20-mmol) amount of salicylaldehyde and 2.48 g (10 mmol) of 2-aminophenyl disulfide were added to 100 mL of an 80:20 (v/v) mixture of MeOH and DMF. The reaction mixture was refluxed under N_2 for 1 h and then cooled to room temperature. At this point, 2.45 g (10 mmol) of manganese(II) acetate tetrahydrate followed by 0.88 g (20 mmol) of sodium methoxide in 20 mL of degassed MeOH was added, generating a deep red solution. This solution was refluxed for 10 h, after which time the mixture was taken to dryness by flash evaporation. The red solid was redissolved in 80 mL of THF, the undissolved sodium acetate was removed by filtration, and the clear red solution was reduced to 25 mL. At this point, 80 mL of MeOH was added. A red crystalline product slowly precipitated from this mixture and was collected by filtration; yield 65%. Anal. Calcd for $MnC_{28}H_{26}N_2O_4S_2$: C, 58.63; H, 4.53; N, 4.88; S, 11.16; Mn, 9.59. Found: C, 57.88; H, 4.62; N, 4.71; S, 11.06; Mn, 9.30. All elemental analyses were performed by Galbraith Analytical Laboratories, Knoxville, TN. X-ray powder pattern with calculated *d* spacings in brackets (*d* spacings in Å): 9.80 [10.102] (very strong (vs)), 8.00 [8.11] (vs), 7.75 [7.73] (vs), 7.10 [7.07] (weak (w)), 6.20 [6.31] (strong (s)), 5.20 [5.16] (very weak (vw)), 5.00 [5.04] (vw), 4.90 [4.88] (vw), 4.20 [4.22] (medium (m)), 4.00 [4.06] (w), 3.90 [3.92] (w), 3.50 [3.48] (m), 3.45 [3.43] (s), 3.35 [3.36] (w), 3.25 [3.24] (m), 3.15 [3.17] (vw), 3.08 [3.09] (s). Major IR bands (3400–400 cm^{-1}): 3301 (w), 3054 (w), 2999 (vw), 2928 (vw), 2884 (vw), 1604 (vs), 1573 (s), 1529 (vs), 1456 (vs), 1439 (vs), 1382 (s), 1344 (m), 1316 (m), 1274 (vw), 1244 (w), 1223 (vw), 1175 (vs), 1148 (vs), 1125 (s), 1057 (vw), 1032 (s), 999 (s), 979 (w), 918 (s), 852 (s), 798 (m), 761 (vs), 751 (vs), 641 (vw), 592 (w), 557 (vw), 543 (w), 530 (w), 506 (w), 482 (s), 460 (w), 444 (w).

Method 2. A 2.16-mL (20-mmol) amount of salicylaldehyde and 2.5 g (20 mmol) of 2-aminothiophenol were refluxed under nitrogen for 1 h in 100 mL of MeOH. After the reaction mixture was cooled to room temperature, 0.88 g (20 mmol) of sodium methoxide and 2.45 g (10 mmol) of manganese(II) acetate tetrahydrate, dissolved in 20 mL of degassed MeOH, were added to the solution. An orange solid precipitated immediately. After the mixture was stirred for 15 min, the orange solid was collected by filtration under a nitrogen atmosphere. The solid was air-sensitive, changing from orange to red-brown. The red-brown solid was partially soluble in THF, giving a deep red solution. A red microcrystalline product can be recovered by addition of MeOH; yield 40%.

Method 3. A 4.56-g (10-mmol) amount of SALPS was dissolved in an 80:20 (v/v) mixture of MeOH and DMF. To this solution was added 0.88 g (20 mmol) of sodium methoxide and 2.45 g (10 mmol) of manganese(II) acetate tetrahydrate. The solution was then refluxed for 10 h. A white solid was removed by vacuum filtration, leaving a dark red solution. The filtrate volume was reduced to 25 mL followed by addition of 80 mL of MeOH. A red crystalline product was collected by filtration; yield 65%.

Table I. Crystallographic Data for Mn(SALPS)CH_3OH and $[Mn(SALPS)]_2$

	Mn(SALPS)CH_3OH·CH_3OH	$[Mn(SALPS)]_2$·$2CH_3CN$
formula	$H_{26}C_{28}N_2O_4S_2Mn$	$H_{42}C_{56}N_6O_4S_4Mn_2$
mol wt	573.6	1101.1
a, Å	9.692 (2)	12.311 (9)
b, Å	11.195 (4)	14.818 (6)
c, Å	13.399 (5)	15.141 (5)
α, deg	110.47 (3)	109.99 (3)
β, deg	94.57 (3)	84.76 (5)
γ, deg	98.95 (3)	103.33 (5)
V, Å^3	1331.2 (9)	2525 (3)
cryst syst	triclinic	triclinic
space group	$P\bar{1}$	$P\bar{1}$
d_{calcd}, g/cm^3	1.431	1.448
d_{obsd},[a] g/cm^3	1.42	1.42
Z	2	2
radiation	Mo Kα (0.701 69 Å)	Mo Kα (0.701 69 Å)
abs coeff, μ, cm^{-1}	6.62	6.90
cryst habit	parallelepiped	block
temp, K	295	235
cryst size, mm	0.149 × 0.161 × 0.460	0.379 × 0.103 × 0.409
scan speed, deg/min	2.5–12	2.5–12
scan range, deg	1.7	1.7
bkgd/scan time ratio	0.8	0.8
octants	$h,\pm k,\pm l$	$h,\pm k,\pm l$
data collected	3502	5082
no. of unique data ($I > 3\sigma(I)$)	2984	3596
no. of variables	358	352
goodness of fit[b]	0.69	1.69
R, %	0.029	0.040
R_w, %	0.031	0.038

[a] Determined by flotation in CCl_4/toluene. [b] Goodness of fit = $[\sigma(w(F_o - F_c)^2)]^{1/2}/\sigma(w)$.

All three synthetic methods gave material with identical X-ray powder patterns and IR spectra. Single-crystal X-ray diffraction studies were completed with a compound synthesized by method 2.

(b) [Mn(SALPS)]$_2$·$2CH_3CN$. A 5.73-g (10-mmol) amount of Mn(SALPS)CH_3OH was added to 100 mL of degassed CH_3CN with stirring. A purple solid precipitated from this solution after 10 min. The purple solid was redissolved in 50 mL of benzene, and 10 mL of CH_3CN was added. Purple crystals deposited upon standing overnight; yield 90%. Anal. Calcd for $Mn_2C_{54}H_{42}N_6O_4S_4$: C, 61.09; H, 3.81; N, 7.63; Mn, 10.0. Found: C, 61.46; H, 3.81; N, 7.05; Mn, 9.90. X-ray powder pattern with calculated *d* spacings in brackets (*d* spacings in A): 13.00 [13.60] (s), 9.00 [9.14] (vs), 7.25 [7.39] (m), 6.60 [6.84] (m), 6.00 [6.15] (vw), 5.50 [5.58] (vw), 4.90 [4.79] (vw), 4.65 [4.54] (m), 4.30 [4.39] (m), 4.05 [4.00] (s), 3.90 [3.88] (m), 3.70 [3.76] (m), 3.60 [3.58] (vw), 3.45 [3.40] (vw), 3.30 [3.36] (vw), 3.10 [3.13] (vw), 3.00 [3.03] (vw), 2.80 [2.84]. Major IR absorption bands (3400–400 cm^{-1}): 3056 (w), 3007 (vw), 2888 (vw), 1608 (vs), 1573 (s), 1545 (m), 1525 (m), 1462 (s), 1453 (s), 1440 (vs), 1383 (m), 1359 (w), 1334 (w), 1293 (s), 1268 (w), 1246 (w), 1225 (w), 1180 (m), 1155 (m), 1147 (s), 1126 (m), 1038 (w), 920 (m), 851 (m), 797 (m), 753 (vs), 643 (vw), 590 (w), 546 (w), 531 (w), 511 (w), 487 (w), 442 (vw), 410 (w).

Collection and Reduction of X-ray Data. Suitable crystals of Mn(SALPS)CH_3OH·CH_3OH and $[Mn(SALPS)]_2$·$2CH_3CN$ were obtained as described above. Crystals were mounted in glass capillaries and sealed under nitrogen. Diffraction experiments were performed at 22 °C for Mn(SALPS)CH_3OH and at −38 °C for $[Mn(SALPS)]_2$ by using liquid-nitrogen boiloff on a Syntex $P2_1$ diffractometer. Intensity data were obtained with Mo Kα radiation monochromatized from a graphite crystal whose diffraction vector was parallel to the diffraction vector of the sample. Three standard reflections were measured every 50 reflections. The crystal and machine parameters used in the unit cell determination and in data acquisition are summarized in Table I. Intensity data were collected from $\theta/2\theta$ scans with $0 < 2\theta < 45°$ for Mn(SALPS)CH_3OH·CH_3OH and $0 < 2\theta < 40°$ for $[Mn(SALPS)]_2$·$2CH_3CN$. Empirical absorption corrections were applied to both data sets. The data were reduced by using the SHELX program package.[16] The structures were solved by using the direct-methods program MULTAN.[17] Atomic

(13) Seela, J. L.; Folting, K.; Wang, R.-J.; Huffman, J. C.; Christou, G.; Chang, H.-R.; Hendrickson, D. N. *Inorg. Chem.* **1985**, *24*, 4454.

(14) (a) Costa, T.; Dorfman, J. R.; Hagen, K. S.; Holm, R. H. *Inorg. Chem.* **1983**, *22*, 4091. (b) Rao, C. P.; Dorfman, J. R.; Holm, R. H. *Inorg. Chem.* **1986**, *25*, 428.

(15) Abbreviations used: SALPS = *N,N'*-[1,1'-dithiobis(phenylene)]bis(salicylideneaminato); SALEN = *N,N'*-ethylenebis(salicylideneaminato); SALDAES = *N,N'*-[2,2'-thiobis(ethanediyl)]bis(salicylideneaminato); SALPN = *N,N'*-(1,2-propanediyl)bis(salicylideneaminato); SALDPT = *N,N'*-[3,3'-iminobis(propyl)]bis(salicylideneaminato); SALDIEN = *N,N'*-[2,2'-iminobis(ethyl)]bis(salicylideneaminato); SNO = *N*-(2-mercaptophenyl)salicylideneaminato MBP = 2,6-bis(2-methyl-2-benzothiazolinyl)pyridine; SDTO = *N,N'*-(3,6-dithiaoctane-1,8-diyl)bis(salicylideneaminato); TREN = tris(2-aminoethyl)amine.

(16) Sheldrick, G. M. "SHELX", program for crystal structure determination, 1976.

scattering factors were from ref. 18. For the solvent molecules of Mn(SALPS)CH_3OH·CH_3OH hydrogen atom positions were refined. In all other cases hydrogen atoms were located but not refined and placed at fixed distances from bonded C atoms of 0.95 Å in the final least-squares refinement. One of the acetonitrile solvates is disordered in the [Mn(SALPS)]$_2$ structure. Therefore, the structure has been refined by using a model with this acetonitrile assigned 0.7 and 0.3 occupancy factors in the two nonoverlapping positions, respectively. Unique data used and final R indices are given in Table I.

Electrochemical Measurements. Electrochemical measurements were performed with a BAS-100 electrochemical analyzer. Cyclic voltammetric measurements were performed at 23 ± 2 °C in the designated solvent under argon with the electroactive component at 10^{-3} M. Tetra-*n*-butylammonium hexafluorophosphate (0.1 M) was used as the supporting electrolyte. A three-electrode configuration was employed, with Ag/AgCl reference and platinum working and auxiliary electrodes. The ferrocene/ferrocenium couple (+400 mV vs. Ag/AgCl) was used as an external standard. Acetonitrile, DMF, and methylene chloride were high-purity solvents purchased from Burdick and Jackson and used as received. All solvents were stored under dry nitrogen.

Spectroscopic Methods. UV/vis spectra were recorded on a Perkin-Elmer Lambda 9 UV/vis/near-IR dual-beam spectrophotometer equipped with a Perkin-Elmer 3600 Data Station to analyze the data. Infrared spectra were recorded on a Nicolet 60 SX Fourier transform infrared spectrophotometer with samples prepared as KBr pellets. Solution and solid-state EPR spectra were recorded on a Bruker ER200 E-SRC spectrometer equipped with a Varian variable-temperature controller. DPPH (g = 2.0037) was used as an external standard.

Magnetic Measurements. Room-temperature magnetic moments were calculated from data obtained with a Faraday balance composed of a Cahn/Ventron R-100 electronic balance and a Varian Fieldial Mark I field-regulated magnetic power supply. The standard used was Hg[Co(SCN)$_4$]. Variable-temperature data were collected on an SHE computer-controlled variable-temperature SQUID susceptometer[19] over the temperature range 1.932–298 K. The value of the exchange constant, J, was determined by the best fit of the data to the Van Vleck equation[20] for a $^5/_2$–$^5/_2$ spin-coupled binuclear system.

Results and Discussion

Synthesis and Reactivity of Complexes. The synthesis of Mn(SALPS)CH_3OH can be achieved by following three distinct paths. First, the compound can be made via the pseudo template reaction of manganese(II) acetate with salicylaldehyde and 2-aminophenyl disulfide in methanol. This reaction gives the highest yields of Mn(SALPS)CH_3OH. Second, synthesis can occur via the aerial oxidation of the highly air sensitive, yellow-orange solid of $Mn^{II}(SNO)_2$[15] in methanol. This reaction proceeds rapidly at room temperature, without an intermediate higher oxidation state manganese species being detected. Third, the compound can be produced through the direct reaction of manganese (II) acetate with SALPS in methanol.

Mn(SALPS)CH_3OH is very slightly soluble in methanol, with crystals suitable for X-ray analysis forming overnight. When Mn(SALPS)CH_3OH is dissolved in DMF, the coordinated methanol is displaced by the solvent, giving the monomeric DMF adduct. The formation of the dimeric material [Mn(SALPS)]$_2$ from the monomeric complex is facile and reversible. Acetonitrile, toluene, benzene, and methylene chloride act as solvents that will afford this transformation. When [Mn(SALPS)]$_2$ is redissolved in DMF, the monomeric material is regenerated.

The tendency for Mn(II) to be six-coordinate is effectively illustrated by the complexes of Mn(II)–SALPS. In methanol, DMF, and pyridine, monomeric materials are recovered that contain one solvent molecule in the manganese coordination sphere. In methylene chloride, acetonitrile, and toluene, the Mn(SALPS) unit dimerizes via phenolate oxygen atoms to attain six-coordination. The strength of this association is substantial as there is no evidence for a monomer/dimer equilibrium in toluene, benzene, acetonitrile, or methylene chloride. Furthermore, the Mn–O(phenolate) bridge bonds are nearly identical, even though

Table II. Atomic Coordinates for Mn(SALPS)CH_3OH·CH_3OH

atom	x	y	z	U_{eq},[a] Å^2
Mn1	0.1966 (1)	0.5658 (1)	0.6783 (1)	0.0296
S1	0.1205 (1)	0.8549 (1)	0.9205 (1)	0.0530
S2	0.0800 (1)	0.7857 (1)	0.7545 (1)	0.0422
O1	0.0181 (2)	0.4227 (2)	0.6375 (1)	0.0379
O2	0.3601 (2)	0.4678 (2)	0.6696 (1)	0.0384
N1	0.1778 (2)	0.5717 (2)	0.8470 (2)	0.0331
N2	0.3699 (2)	0.7392 (2)	0.7081 (2)	0.0303
C1	−0.0268 (3)	0.3404 (3)	0.6836 (2)	0.0345
C2	−0.1268 (3)	0.2253 (3)	0.6220 (2)	0.0393
C3	−0.1810 (3)	0.1379 (3)	0.6677 (3)	0.0448
C4	−0.1380 (3)	0.1587 (3)	0.7748 (3)	0.0508
C5	−0.0383 (3)	0.2680 (3)	0.8359 (2)	0.0442
C6	0.0186 (3)	0.3605 (3)	0.7930 (2)	0.0329
C7	0.1180 (3)	0.4731 (3)	0.8666 (2)	0.0371
C8	0.2810 (3)	0.6684 (3)	0.9284 (2)	0.0344
C9	0.3963 (3)	0.6357 (3)	0.9728 (2)	0.0448
C10	0.5031 (3)	0.7318 (4)	1.0470 (2)	0.0542
C11	0.4946 (4)	0.8607 (4)	1.0753 (3)	0.0556
C12	0.3807 (4)	0.8953 (3)	1.0311 (2)	0.0513
C13	0.2717 (3)	0.8010 (3)	0.9580 (2)	0.0392
C14	0.2061 (3)	0.8848 (3)	0.7126 (2)	0.0340
C15	0.1720 (3)	0.9944 (3)	0.6977 (2)	0.0464
C16	0.2632 (4)	1.0660 (3)	0.6562 (3)	0.0529
C17	0.3873 (3)	1.0271 (3)	0.6275 (2)	0.0482
C18	0.4241 (3)	0.9190 (3)	0.6427 (2)	0.0382
C19	0.3352 (3)	0.8487 (2)	0.6889 (2)	0.0301
C20	0.5002 (3)	0.7447 (3)	0.7423 (2)	0.0303
C21	0.5584 (3)	0.6431 (3)	0.7624 (2)	0.0331
C22	0.6960 (3)	0.6795 (3)	0.8206 (2)	0.0398
C23	0.7610 (3)	0.5909 (3)	0.8474 (2)	0.0473
C24	0.6888 (3)	0.4632 (3)	0.8158 (2)	0.0476
C25	0.5550 (3)	0.4232 (3)	0.7577 (2)	0.0412
C26	0.4860 (3)	0.5107 (3)	0.7279 (2)	0.0322
O3	0.1691 (2)	0.5647 (2)	0.5150 (1)	0.0425
C27	0.2882 (4)	0.5570 (4)	0.4582 (3)	0.0523
O4	0.3353 (3)	0.2372 (2)	0.4910 (2)	0.0625
C28	0.2003 (5)	0.2172 (4)	0.4395 (4)	0.0657

[a] U_{eq} is defined as one-third of the trace of the U_{ij} tensor.

[Mn(SALPS)]$_2$ does not contain crystallographically imposed symmetry.

Many Mn(II) Schiff base complexes[21-26] form air-sensitive solutions and solids. This is true of the yellow solid $Mn^{II}(SNO)_2$, which can act as a precursor to the monomeric Mn(SALPS)(solvent). In contrast, both Mn(SALPS)(solvent) and [Mn(SALPS)]$_2$ form air-stable solutions and are unreactive toward dioxygen in the solid state. This is undoubtedly due to the rather positive redox potentials exhibited by both complexes. This conclusion is fully supported by the work of Coleman and Taylor,[23] in which the redox potentials of Mn(II) complexes were correlated with dioxygen reactivity. Another dianionic pentadentate ligand that contains two thiolate sulfur atoms, MBP,[15,27] has been formulated as an air-stable Mn(II) complex while the dithioether sexidentate ligand SDTO[15,27] only forms an Mn(III) complex. It is obvious from these and other studies that the factors governing stable manganese(III) complexes with sulfur are still poorly understood.

Attempts to isolate $Mn^{III}(SALPS)^+$, either by direct reaction of manganese(III) acetate with SALPS or via chemical or electrochemical oxidation of Mn(SALPS)CH_3OH, were unsuccessful. Similarly, all attempts to oxidize [Mn(SALPS)]$_2$ were also unsuccessful, suggesting that this material is stable only as the (II/II)

(17) Main, P. "MULTAN78", program for crystal structure determination, 1978.
(18) *International Tables for X-ray Crystallography*; Kynoch: Birmingham, England, 1974; Vol. 4.
(19) SHE. Corp, San Diego, CA 92121.
(20) Wojciechowski, W. *Inorg. Chim. Acta* **1967**, *1*, 319.
(21) Coleman, W. M.; Taylor, L. T. *Inorg. Chem.* **1977**, *16*, 1114.
(22) Pecoraro, V. L.; Butler, W. M. *Acta Crystallogr., Sect. C: Cryst. Struct. Commun.* **1986** *C42*, 1151.
(23) Coleman, W. M.; Boggess, R. K.; Hughes, J. W.; Taylor, L. T. *Inorg. Chem.* **1981**, *20*, 700.
(24) Coleman, W. M.; Taylor, L. T. *Coord. Chem. Rev.* **1980**, *32*, 1.
(25) McAuliffe, C. A.; Al-Khateeb, H.; Jones, M. H.; Levason, W.; Minten, K.; McCulough, J. *J. Chem. Soc., Chem. Commun.* **1979**, 736.
(26) Cini, R.; Zanello, P.; Cinquantini, A.; Colligiani, A.; Pinzino, C.; Valentini, G. *Inorg. Chim. Acta* **1984**, *88*, 105.
(27) Bryan, P. S.; Stone, C. K. *Inorg. Nucl. Chem. Lett.* **1977**, *13*, 581.

Table III. Atomic Coordinates for $[Mn(SALPS)]_2 \cdot 2CH_3CN$

atom	x	y	z	U_{eq}, Å^2	atom	x	y	z	U_{eq}, Å^2
Mn1	0.3367 (1)	0.0996 (1)	0.3082 (1)	0.0267	C29	0.2000 (5)	0.0313 (5)	0.5928 (4)	0.0417
Mn2	0.1961 (1)	−0.1280 (1)	0.2132 (1)	0.0267	C30	0.1072 (5)	−0.0392 (5)	0.6016 (4)	0.0434
O1	0.3403 (3)	−0.0283 (2)	0.1879 (2)	0.0284	C31	0.0484 (5)	−0.0982 (4)	0.5219 (4)	0.0378
C1	0.4359 (5)	−0.0432 (4)	0.1431 (4)	0.0293	C32	0.0796 (5)	−0.0913 (4)	0.4328 (4)	0.0295
C2	0.4587 (5)	−0.1380 (4)	0.1120 (4)	0.0446	C33	0.0057 (4)	−0.1545 (4)	0.3570 (4)	0.0292
C3	0.5575 (6)	−0.1551 (5)	0.0645 (5)	0.0514	N3	0.0208 (4)	−0.1670 (3)	0.2687 (3)	0.0293
C4	0.6364 (5)	−0.0799 (5)	0.0466 (4)	0.0429	C34	−0.0642 (5)	−0.2360 (4)	0.2067 (4)	0.0299
C5	0.6236 (5)	0.0127 (4)	0.0745 (4)	0.0362	C35	−0.1013 (5)	−0.3302 (5)	0.2141 (4)	0.0407
C6	0.5155 (4)	0.0332 (4)	0.1237 (4)	0.0262	C36	−0.1847 (6)	−0.3973 (5)	0.1526 (6)	0.0504
C7	0.5047 (4)	0.1331 (4)	0.1501 (4)	0.0312	C37	−0.2259 (6)	−0.3718 (6)	0.0869 (6)	0.0572
N1	0.4314 (4)	0.1734 (3)	0.2070 (3)	0.0289	C38	−0.1866 (06)	−0.2808 (06)	0.0772 (05)	0.0493
C8	0.4458 (5)	0.2778 (4)	0.2288 (4)	0.0331	C39	−0.1070 (05)	−0.2129 (04)	0.1382 (04)	0.0363
C9	0.5503 (5)	0.3379 (5)	0.2584 (4)	0.0408	S3	−0.0759 (01)	0.0929 (01)	0.1294 (01)	0.0463
C10	0.5620 (6)	0.4396 (5)	0.2861 (4)	0.0508	S4	0.0932 (01)	−0.0602 (01)	0.1060 (01)	0.0363
C11	0.4738 (8)	0.4804 (5)	0.2868 (5)	0.0595	C40	0.1156 (05)	−0.1462 (04)	−0.0056 (04)	0.0314
C12	0.3703 (6)	0.4218 (5)	0.2580 (5)	0.0578	C41	0.0970 (05)	−0.1277 (05)	−0.0860 (05)	0.0445
C13	0.3560 (5)	0.3197 (5)	0.2287 (4)	0.0415	C42	0.1236 (05)	−0.1881 (05)	−0.1737 (04)	0.0458
S1	0.2238 (1)	0.2501 (1)	0.1820 (1)	0.0490	C43	0.1689 (05)	−0.2666 (05)	−0.1798 (04)	0.0415
S2	0.1641 (1)	0.1716 (1)	0.2720 (1)	0.0336	C44	0.1867 (05)	−0.2872 (04)	−0.1001 (04)	0.0348
C14	0.1586 (5)	0.2650 (4)	0.3824 (4)	0.0273	C45	0.1568 (04)	−0.2292 (04)	−0.0120 (04)	0.0283
C15	0.0693 (5)	0.3121 (4)	0.4043 (4)	0.0366	N4	0.1685 (03)	−0.2487 (03)	−0.0722 (03)	0.0283
C16	0.0596 (5)	0.3781 (4)	0.4929 (5)	0.0429	C46	0.1462 (04)	−0.3403 (04)	0.0663 (04)	0.0317
C17	0.1364 (6)	0.3951 (4)	0.5612 (4)	0.0399	C47	0.1497 (4)	−0.3789 (4)	0.1401 (4)	0.0327
C18	0.2260 (5)	0.3494 (4)	0.5396 (4)	0.0348	C48	0.1007 (5)	−0.4807 (4)	0.1224 (5)	0.0469
C19	0.2418 (5)	0.2873 (4)	0.4487 (4)	0.0300	C49	0.0910 (5)	−0.5234 (5)	0.1894 (6)	0.0586
N2	0.3363 (4)	0.2447 (3)	0.4230 (3)	0.0269	C50	0.1316 (6)	−0.4664 (6)	0.2782 (5)	0.0632
C20	0.4297 (5)	0.3017 (4)	0.4568 (4)	0.0308	C51	0.1828 (5)	−0.3690 (5)	0.2995 (4)	0.0487
C21	0.5383 (5)	0.2780 (4)	0.4446 (4)	0.0312	C52	0.1948 (5)	−0.3220 (5)	0.2311 (4)	0.0365
C22	0.6314 (5)	0.3582 (4)	0.4756 (4)	0.0399	O4	0.2464 (3)	−0.2309 (3)	0.2514 (3)	0.0391
C23	0.7375 (5)	0.3442 (5)	0.4657 (4)	0.0468	C61	0.5512 (12)	0.3938 (13)	−0.1305 (08)	0.1207
C24	0.7554 (5)	0.2488 (6)	0.4274 (5)	0.0496	N62	0.5680 (08)	0.4035 (07)	−0.0394 (07)	0.1192
C25	0.6677 (5)	0.1694 (5)	0.3965 (4)	0.0463	C63	0.6049 (11)	0.4010 (08)	0.0306 (10)	0.0700
C26	0.5571 (5)	0.1807 (5)	0.4029 (4)	0.0370	C71	0.5350 (09)	0.1142 (07)	0.6157 (07)	0.1020
O2	0.4763 (3)	0.1039 (3)	0.3731 (3)	0.0394	N72	0.4765 (11)	0.1920 (08)	0.6437 (07)	0.1450
O3	0.2081 (3)	−0.0073 (2)	0.3421 (2)	0.0270	C73	0.4278 (11)	0.2597 (07)	0.6657 (08)	0.0815
C27	0.1753 (5)	−0.0191 (4)	0.4240 (4)	0.0305	C81	0.4946 (16)	0.4436 (14)	0.0568 (12)	0.0300
C28	0.2334 (5)	0.0422 (4)	0.5072 (4)	0.0340	C82	0.5504 (18)	0.4814 (15)	−0.0870 (15)	0.0341

Table IV. Selected Interatomic Distances (Å) and Angles (deg) for $Mn(SALPS)CH_3OH \cdot CH_3OH$

Mn1–S2	2.769 (1)	Mn1–N1	2.261 (2)		
Mn1–O1	2.057 (2)	Mn1–N2	2.255 (2)		
Mn1–O2	2.052 (2)	Mn1–O3	2.178 (2)		
Mn1–S1	3.914 (2)	S1–S2	2.065 (1)		
S2–Mn1–O1	100.4 (1)	S2–Mn1–O2	152.9 (1)	S2–Mn1–O3	91.4 (1)
S2–Mn1–N1	80.8 (1)	S2–Mn1–N2	72.8 (1)	O1–Mn1–O2	104.3 (1)
O1–Mn1–N1	83.4 (1)	O1–Mn1–N2	170.1 (1)	O1–Mn1–O3	89.2 (1)
O2–Mn1–N1	91.1 (1)	O2–Mn1–N2	83.9 (1)	O2–Mn1–O3	99.8 (1)
O3–Mn1–N1	168.1 (1)	O3–Mn1–N2	83.8 (1)	N1–Mn1–N2	102.2 (1)

dimer. Whether the instability of the mixed-valence (II/III) complex is simply due to the dissociation of Mn(SALPS) units or due to ligand-centered oxidation is unclear. However, since the monomeric Mn(SALPS)(solvent) is also unstable to oxidation, the ligand itself may decompose under oxidizing conditions, possibly forming oxidized sulfur species as has been described in Au(III)–disulfide chemistry.[28]

Description of Structures. Parameters for data collection are given in Table I. Fractional atomic coordinates for $Mn(SALPS)CH_3OH$ and $[Mn(SALPS)]_2$ are given in Tables II and III, respectively. The structure of $Mn(SALPS)CH_3OH$ is very similar to that of the previously reported $Fe^{III}(SALPS)Cl$.[29] In both cases, the high-spin d^5 metal ion is six-coordinate in what must be described as a highly distorted octahedron. As illustrated in Figure 1, SALPS acts as a pentadentate ligand supplying two imine nitrogens, two phenolate oxygens, and one disulfide sulfur as coordinating groups. The sixth coordination site is occupied by an oxygen atom from methanol. Only one of the disulfide sulfur atoms (S2) is in bonding distance (Mn1–S2 = 2.769 Å (Table IV)), with the Mn1–S1 distance being nearly 4 Å. The S1–S2 distance is 2.065 Å, which is in good agreement with the distance reported for Fe(SALPS)Cl and other structures containing di-

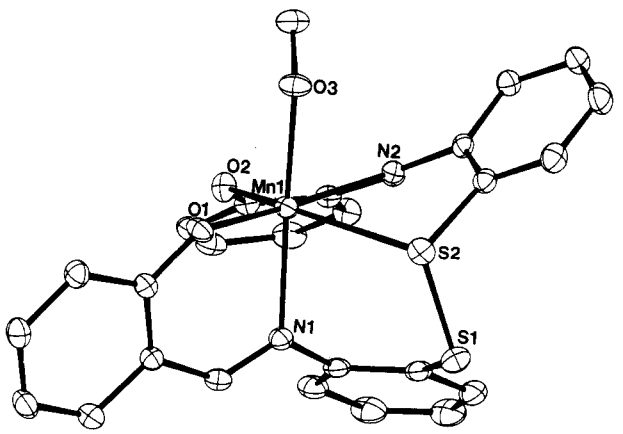

Figure 1. ORTEP plot of $Mn(SALPS)CH_3OH$, with numbering scheme around the Mn atom, as viewed perpendicular to the Mn–O (CH_3OH) bond axis (25% probability ellipsoids).

(28) Shaw, F., III; Cancrou, P. L.; Witkiewicz, P. L.; Eldrich, J. A. *Inorg. Chem.* **1980**, *19*, 3198.
(29) Bertrand, J. A.; Breece, J. L. *Inorg. Chim. Acta* **1974**, *8*, 267.

Table V. Selected Interatomic Distances (Å) and Angles (deg) for $[Mn(SALPS)]_2 \cdot 2CH_3CN$

Mn1–O1	2.140 (3)	Mn1–O2	2.034 (4)	Mn1–O3	2.129 (3)
Mn1–N1	2.266 (5)	Mn1–N2	2.257 (4)	Mn1–S2	2.757 (2)
Mn2–O1	2.130 (3)	Mn2–O4	2.036 (5)	Mn2–O3	2.139 (3)
Mn2–N3	2.264 (4)	Mn2–N4	2.262 (4)	Mn2–S4	2.707 (2)
Mn1–Mn2	3.300 (1)	Mn1–S1	3.929 (3)	Mn2–S3	3.887 (3)
S1–S2	2.064 (3)	S3–S4	2.052 (2)		
S2–Mn1–O1	103.7 (1)	S2–Mn1–O2	156.3 (1)	S2–Mn1–O3	85.1 (1)
S2–Mn1–N1	82.8 (1)	S2–Mn1–N2	72.8 (1)	S1–S2–Mn1	108.0 (1)
O1–Mn1–O2	99.1 (1)	N1–Mn1–N2	92.6 (2)	O1–Mn1–N1	81.0 (1)
O1–Mn1–N2	173.2 (2)	Mn1–O1–Mn2	101.2 (1)	O2–Mn1–N1	94.4 (2)
O2–Mn1–N2	83.8 (2)	O2–Mn1–O3	106.2 (2)	O3–Mn1–N1	152.7 (1)
O3–Mn1–N2	107.1 (1)	O1–Mn1–O3	78.2 (1)	O1–Mn2–O3	78.2 (1)
O3–Mn2–O4	102.3 (2)	O3–Mn2–N3	81.7 (1)	O3–Mn2–N4	173.5 (2)
O3–Mn2–S4	99.9 (1)	Mn1–O3–Mn2	101.3 (1)	N3–Mn2–S4	83.1 (2)
O1–Mn2–O4	108.6 (2)	O1–Mn2–N3	153.8 (2)	O1–Mn2–N4	102.8 (1)
O1–Mn2–S4	83.9 (1)	S4–Mn2–N4	73.9 (1)	S4–Mn2–N4	73.9 (1)
S4–Mn2–O4	156.3 (1)	S3–S4–Mn2	108.8 (1)	O4–Mn2–N4	83.5 (2)
O4–Mn2–N3	92.0 (2)	N3–Mn2–N4	95.3 (1)		

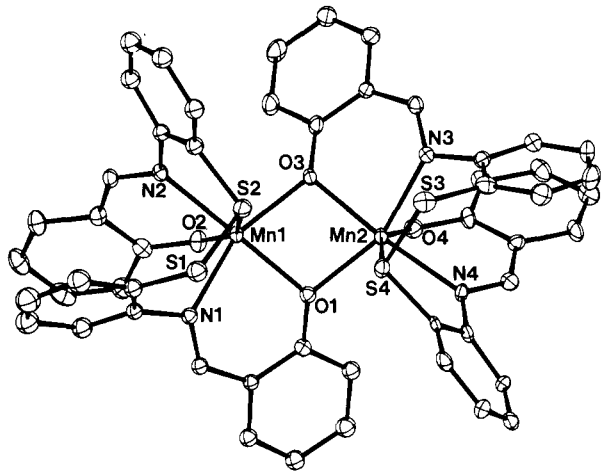

Figure 2. ORTEP plot of $[Mn(SALPS)]_2$, with numbering scheme around the Mn atoms, as viewed down the pseudo-2-fold axis (25% probability ellipsoids).

sulfides.[29-32] As expected, the Mn1–S2 distance is significantly longer than the Mn–S distance for Mn(II)–thiolate coordination,[33] 2.4 Å. Mn–O and Mn–N bonds are the expected length as based on other Mn(II) Schiff base structures. The Mn–O3(methanol) bond is over 0.1 Å longer than the phenolate oxygen bonds, reflecting the weaker association of methanol to the manganese.

Besides the asymmetry in bond lengths observed for the metal coordination sphere, there are marked deviations from 90° for the bond angles at the manganese ion. Bond angles for cis substituents range between 72.8° for S2–Mn1–N2 and 104.3° for O1–Mn1–O2. Similarly, the angle described by the trans ligands O2 and S2 is only 152.9°. The EPR spectrum of this material, discussed below, directly reflects the asymmetric nature of this complex.

Selected interatomic distances and angles for $[Mn(SALPS)]_2$ are reported in Table V. The SALPS dianionic ligand once again acts as a pentadentate chelating agent. By dissolution of the monomer in acetonitrile, the methanol has been displaced by a phenolate oxygen atom from another Mn(SALPS) unit. This results in the diphenoxy-bridged dimer, illustrated in Figure 2, which can be considered as two edge-sharing octahedra. Dimerization via phenolate oxygen atoms is common in SALEN structures such as $[Cu(SALEN)]_2$,[33] $[Fe(SALEN)Cl]_2$,[34] and $[Co(SALEN)X]_2$.[35] It has also been proposed for $Mn^{II}(SALEN)$[36] and $Mn^{III}(SALEN)Br$[37] on the basis of magnetic data. The X-ray structure of a monomeric $Mn^{III}(SALEN)Cl$[22] has appeared; however, other diphenoxy-bridged Mn(III) Schiff base complexes have been structurally characterized.[38,39]

Table VI. Spectral and Electrochemical Data for Mn(SALPS)MeOH and $[Mn(SALPS)]_2$

solvent	λ_{max} nm	log ϵ	E_{Pa}[a,b]	E_{Pc}[a,b]
	Mn(SALPS)MeOH			
CH_2Cl_2	370	4.39[c]	625	
	418	4.23[c]		402
				838
				720
DMF	409	4.16[d]	532	120
PYR	350	4.23[d]		
	$[Mn(SALPS)]_2$			
CH_2Cl_2	389	4.37[d]	598	
	427	4.32[d]		474
			823	
				747
toluene	393	4.34[c]		
	432	4.30[c]		
DMF	409	4.16[d]	470	69
PYR	350	4.22[d]		

[a] Scan rate 0.15 V s^{-1}. [b] Potentials reported in mV vs. Ag/AgCl with the ferrocene/ferrocenium couple as an external standard. [c] log ϵ per dimer. [d] log ϵ per monomer.

The Mn–N and Mn–S bond lengths remain essentially unchanged on going from $Mn(SALPS)CH_3OH$ to $[Mn(SALPS)]_2$; however, there are marked differences in Mn–O bond lengths that result from the modification of the role of the phenolate oxygen atoms in the structure. While terminally coordinated phenolates O2 and O4 show a slight shortening of the bond length to manganese, the two phenolate oxygens O1 and O3, which act as bridging ligands between Mn1 and Mn2, have substantially longer bond lengths. In both cases, the bridging phenolate oxygen atoms are trans to imine nitrogen atoms. The manganese atoms in the dimer are separated by 3.300 Å.

The dimer has been formed so as to orient both disulfide linkages on the same side of the molecule. This orientation gives rise to the crystallographically nonrigorous twofold axis seen in Figure 2. The greatest change in cis bond angles as one goes from the monomer to the dimer is observed for the pair N2–Mn1–O3 (107.1°) and N4–Mn2–O1 (102.8°), which relate to O3–Mn1–N2

(30) Branden, C. I. *Acta Chem. Scand.* **1967**, *21*, 1000.
(31) Bonds, W. D., Jr.; Ibers, J. A. *J. Am. Chem. Soc.* **1972**, *94*, 3415.
(32) Riley, P. E.; Seff, K. *Inorg. Chem.* **1972**, *11*, 2993.
(33) Watson, A. D.; Pulla Rao, C. H.; Dorfman, J. R.; Holm, R. H. *Inorg. Chem.* **1985**, *24*, 2820.
(34) Hall, D.; Waters, T. N. *J. Chem. Soc.* **1960**, 2644.
(35) Gerloch, M.; Mabbs, F. E. *J. Chem. Soc. A* **1967**, 1900.
(36) Calligaris, M.; Minichell, D.; Nardin, G.; Randaccio, L. *J. Chem. Soc. A* **1971**, 2720.
(37) Earnshaw, A.; King, E. A.; Larknorthy, L. F. *J. Chem. Soc. A* **1968**, 1048.
(38) Kennedy, B. J.; Murray, K. S. *Inorg. Chem.* **1985**, *24*, 1552.
(39) Vincent, J. B.; Folting, K.; Huffman, J. C.; Christou, G. *Inorg. Chem.* **1986**, *25*, 996.

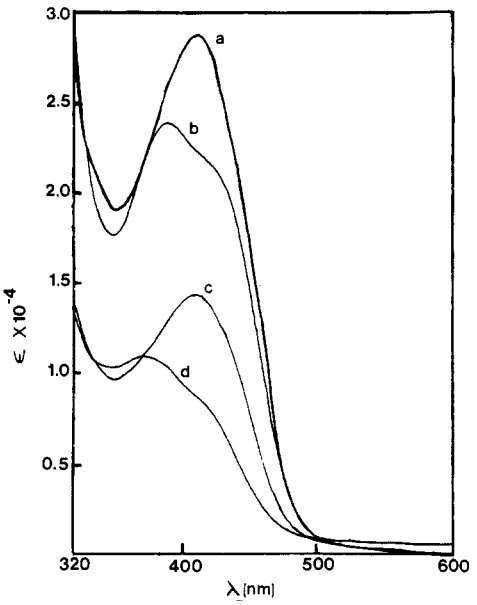

Figure 3. UV/vis spectra of $Mn(SALPS)CH_3OH$ and $[Mn(SALPS)]_2$ dissolved in CH_2Cl_2 or DMF. All spectra are normalized such that the concentration of $Mn(SALPS)CH_3OH$ or $[Mn(SALPS)]_2$ would be 0.1 mM in the absence of dimerization or dissociation, respectively. The actual species present and their concentrations are given in braces: (a) $[Mn(SALPS)]_2$ dissolved in DMF {Mn(SALPS)DMF, 0.2 mM}; (b) $[Mn(SALPS)]_2$ dissolved in CH_2Cl_2 {$[Mn(SALPS)]_2$, 0.1 mM}; (c) $Mn(SALPS)CH_3OH$ dissolved in DMF {Mn(SALPS)DMF, 0.1 mM}; (d) $Mn(SALPS)CH_3OH$ dissolved in CH_2Cl_2 {$[Mn(SALPS)]_2$, 0.05 mM}.

(83.8°) in the monomer. The bridge angles Mn1–(O1 or O3)–Mn2 and O1–(Mn1 or Mn2)–O3 are bracketed by those observed for $[Fe(SALEN)Cl]_2$ (O–Fe–O = 75°; Fe–O–Fe = 105°)[35] and $[Co(SALEN)C_2H_5]_2$ (O–Co–O = 81.2°; Co–O–Co = 98.8°).[34] Both $Mn(SALPS)CH_3OH$ and $[Mn(SALPS)]_2$ contain solvent molecules of crystallization. The methanol solvate in the lattice of the monomeric crystals does not engage in hydrogen bonding. In the case of $[Mn(SALPS)]_2$, the crystals exhibited instability while in the X-ray beam, which may in part be due to the loss of acetonitrile from the lattice. For this reason, data were collected at −38 °C.

UV/Vis Spectra. The UV/vis spectra for $Mn(SALPS)CH_3OH$ and $[Mn(SALPS)]_2$ in DMF and methylene chloride are illustrated as Figure 3. There are two types of spectra, which are defined by the choice of solvent. In DMF, both $Mn(SALPS)CH_3OH$ and $[Mn(SALPS)]_2$ contain one broad absorption at 409 nm. The extinction coefficients (per mole of manganese) for these complexes are given in Table VI. Within experimental error they are identical, suggesting that in DMF solution both $Mn(SALPS)CH_3OH$ and $[Mn(SALPS)]_2$ are converted to the same compound. We believe that DMF either replaces the methanol or cleaves the dimer, respectively, to generate the monomeric Mn(SALPS)DMF complex. Similar behavior is observed in pyridine (PYR); however, the absorption band shifts to higher energy in this case (see Table VI). When pyridine is titrated into a DMF solution of Mn(SALPS)DMF, the spectra shown in Figure 4 are obtained. The isosbestic point at 383 nm demonstrates that Mn(SALPS)DMF and Mn(SALPS)PYR are the only manganese-containing species in solution. The formation constant, K_1, for pyridine binding to Mn(SALPS) in DMF is 3.9 ± 0.5 M^{-1}, where K_1 is defined as

$$K_1 = \frac{[Mn(SALPS)PYR]}{[Mn(SALPS)DMF][PYR]}$$

The spectra of $Mn(SALPS)CH_3OH$ or $[Mn(SALPS)]_2$ are more complex in methylene chloride, where two absorption bands are observed. Once again the spectra are very similar; however, they are not identical as the absorption bands for the solution originating from $Mn(SALPS)CH_3OH$ are at slightly higher energy, although

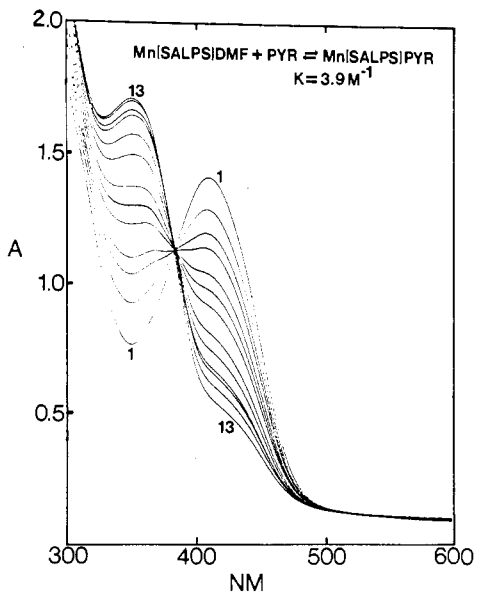

Figure 4. Titration of Mn(SALPS)DMF with pyridine. [Mn(SALPS)] = 9.59 × 10^{-5} M. Ten-microliter aliquots (0.124 mmol) of pyridine were added to an initial 3 mL volume of [Mn(SALPS)DMF] in DMF (spectrum 1). The final spectrum corresponds to 130 μL (1.61 mmol) addition (spectrum 13).

the extinction coefficients are nearly identical. We believe these spectra are indicative of the dimer or a closely related species. We investigated the concentration dependence of the spectra in nondonor solvents to ensure that the spectra did not represent an equilibrium between monomeric and dimeric species. These studies were carried out in toluene due to the greater solubility of $[Mn(SALPS)]_2$ in this solvent. Over a 15-fold range of concentrations both absorption bands obeyed Beer's law, indicating that a monomer/dimer equilibrium did not exist. In all cases, the spectra are consistent with a Mn(II)–Schiff base complex. There is no evidence for an absorption band at lower energy, which is associated with many Mn(III)–Schiff base complexes.[40] The prominent feature observed in DMF at 409 nm is assigned as an intraligand transition as observed for $Mn^{II}(SALPN)$.[41] This absorption band is shifted to higher energy (350 nm) in the spectrum of SALPS. The assignment of these complexes as Mn(II) species is consistent with the room-temperature magnetic moments ($Mn(SALPS)CH_3OH$, 5.94 μ_B/Mn; $[Mn(SALPS)]_2$, 5.90 μ_B/Mn) and EPR spectra discussed below.

Electrochemical Studies. Cyclic voltammograms of $Mn(SALPS)CH_3OH$ and $[Mn(SALPS)]_2$ in DMF and methylene chloride are presented as Figure 5, with peak potentials reported in Table VI. The neutral uncomplexed ligand is not electroactive over the range −1.0 to +1.0 V. The complexes exhibit irreversible electrochemistry regardless of the solvent employed for the measurements. This is established by the greater than 59 mV separation between anodic and cathodic peaks, current ratios that are much greater than 1, and scan-rate-dependent shifts in peak potentials. The electrochemical data lend further support to speciation of Mn(SALPS) in solvents such as DMF relative to methylene chloride. The cyclic voltammograms of Mn(SALPS) are essentially identical in DMF regardless whether $Mn(SALPS)CH_3OH$ or $[Mn(SALPS)]_2$ is used as the source of electroactive material. Thus in DMF, Mn(SALPS)DMF is the electroactive component. A single oxidative wave is seen at about +500 mV (all potentials are vs. Ag/AgCl electrode), followed by a weaker reductive wave at +100 mV. The cyclic voltammogram of Mn(SALPS)DMF is similar to that of the thioether-containing pentadentate Schiff base complex $Mn^{II}(SALDAES)$.[15,23] However, it is more difficult to oxidize the manganese in Mn-

(40) Boucher, L. J.; Coe, C. G. *Inorg. Chem.* **1976**, *15*, 1334.
(41) Okawa, H.; Honda, A.; Nakamura, M.; Kida, S. *J. Chem. Soc., Dalton Trans.* **1985**, 59.

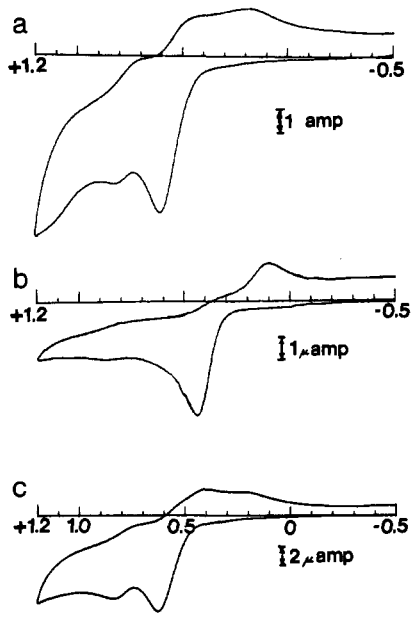

Figure 5. Cyclic voltammograms of $[Mn(SALPS)]_2$ and $Mn(SALPS)CH_3OH$: (a) $[Mn(SALPS)]_2$ dissolved in CH_2Cl_2; (b) $[Mn(SALPS)]_2$ dissolved in DMF; (c) Mn(SALPS)MeOH dissolved in CH_2Cl_2. All electroactive species were at 1×10^{-3} M. Scan rate = 0.15 V s^{-1}. The supporting electrolyte was 0.1 M tri-*n*-butylammonium hexafluorophosphate.

(SALPS)DMF than in Mn(SALDAES).

In solvents where $[Mn(SALPS)]_2$ is the electroactive component, the electrochemical behavior is more complex. In methylene chloride, two oxidative waves (+598 and +823 mV) and three reductive waves (+747, +474, and +190 mV) are seen. We have been unable to isolate stable mixed-valence $Mn^{II/III}(SALPS)_2$ by electrochemical or chemical methods. It appears that upon oxidation both the monomer and dimer decompose. Further characterization of these decomposition products has not been carried out.

EPR Spectroscopy and Magnetic Measurements. The X-band EPR spectra of $Mn(SALPS)CH_3OH$ in DMF/CH_3OH and $[Mn(SALPS)]_2$ in toluene/acetone at 90 K are illustrated in Figure 6. Both spectra are indicative of the highly asymmetric electronic environment of the manganese in these complexes. The monomeric material shows the six-line hyperfine signal at $g = 2$, which is associated with the $I = {}^5/_2$ nuclear spin of ^{55}Mn. The hyperfine coupling constant is 93 G. Superhyperfine coupling, associated with the imine nitrogen atoms, is also apparent. The spectrum is consistent with the observed room-temperature magnetic moment of 5.94 μ_B, which demonstrates that the material is a high-spin Mn(II). As discussed above, the complex is significantly distorted from octahedral symmetry. The highly distorted electronic environment is demonstrated by the many features of the spectrum shown in Figure 6a. In addition to the hyperfine-containing resonance at $g = 2$, a dominant broad resonance is centered at $g = 3$ with other less intense resonances at $g = 1.1$, 6, and 13.8. For complexes with strong axially symmetric electric fields, $\lambda = 0$ ($\lambda = E/D$; $D \neq 0$ and $E = 0$, where D and E are the axial and rhombic zero-field splitting parameters, respectively), effective g values are predicted at $g = 2$ and $g = 6$.[42-48] Such

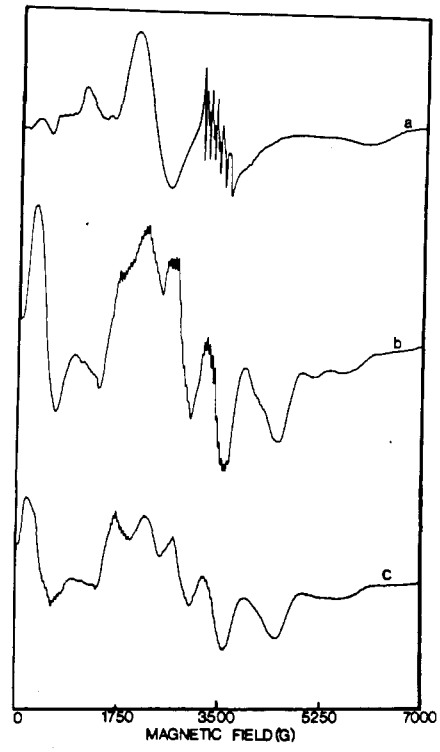

Figure 6. EPR spectra: (a) $Mn(SALPS)CH_3OH$ dissolved in DMF/methanol (1:1) at 90 K (microwave frequency, 9.29 GHz; power, 10 dB; modulator/receiver frequency, 100 KHz; field modulator intensity, 10 G; gain, 25×10^5; time constant, 50 s; Mn nuclear hyperfine coupling, 93 G); (b) $[Mn(SALPS)]_2$ dissolved in acetone/toluene (1:1) at 90 K (microwave frequency, 9.29 GHz; power, 5 dB; modulator/receiver frequency, 100 Hz; field modulator intensity, 10 G; gain, 3.2×10^4; time constant, 50 s); (c) $[Mn(SALPS)]_2$ dissolved in toluene. (spectral conditions as in part B).

spectra have been observed for monomeric Mn(II)–Schiff base complexes,[42] trigonal-bipyramidal amine complexes,[43] and axially distorted MnL_4X_2 (L = picoline (pic); X = Br, I) complexes.[44] In these systems, λ was shown to be close to zero and acceptable fits to the data were obtained with D being 2.17 cm^{-1} ($Mn(5\text{-}NG_2\text{-}SALDPT)\cdot 2H_2O$),[42] 1.41 ($Mn(SALDPT)\cdot 2H_2O$),[42] 0.54 cm^{-1} ($Mn(\gamma\text{-pic})Br_2$), 0.87 cm^{-1} ($Mn(\gamma\text{-pic})I_2$),[44] and 0.24 cm^{-1} ($[Mn(Me_6tren)I]I$).[43] The absence of a single strong resonance at $g_{eff} = 6$ for $Mn(SALPS)CH_3OH$ indicates that this complex does not satisfy a strong axially symmetric electronic environment with $D \geq 0.2$ cm^{-1}. The X-ray structure of the material is consistent with this conclusion as it exhibits a rhombic distortion from octahedral geometry. However, an analysis using purely rhombic symmetry does not seem valid either since $g_{eff} = 4.3$ is predicted when $\lambda = 1/3$ for an $S = {}^5/_2$ system.[47] The spin Hamiltonian[45] usually used to fit $S = {}^5/_2$ systems is

$$H = \beta \mathbf{H}\cdot\mathbf{g}\cdot\mathbf{S} + D[S_z^2 - {}^1/_3 S(S+1)] + E(S_x^2 - S_y^2)$$

The actual g values ($g_\parallel$ and $g_\perp$ for axial symmetry and g_x, g_y, and g_z for rhombic symmetry) are usually quite close to 2[42,43,47,48] so that $g_{eff} = 3$ should result from the zero-field splitting terms. Comparison of the EPR spectrum of $Mn(SALPS)CH_3OH$ with predicted[47] EPR transitions for $S = {}^5/_2$ systems indicate that, whether the system is axial or rhombic, the D value must be 0.1 cm^{-1} or less to observe the strong $g_{eff} = 3$ signal. A more detailed analysis of this spectrum is not presented at this time.

The X-band EPR spectra of the dimer shown in Figure 6b,c are very intriguing. The origin of the complexity has been discussed in detail previously,[42,43] and a number of examples of dimeric Mn(II) complexes are now known.[42,43,49,50] Basically,

(42) Mabad, B.; Cassoux, P.; Tuchagues, J.-P.; Hendrickson, D. N. *Inorg. Chem.* **1986**, *25*, 1420.
(43) Laskowski, E. J.; Hendrickson, D. N. *Inorg. Chem.* **1978**, *17*, 457.
(44) Dowsing, R. D.; Gibson, J. F.; Goodgame, D. M. L.; Goodgame, M.; Hayward, P. J. *J. Chem. Soc. A* **1969**, 187.
(45) Dowsing, R. D.; Gibson, J. F.; Goodgame, M.; Hayward, P. J. *J. Chem. Soc. A* **1969**, 1242.
(46) Goodgame, D. M. L.; Goodgame, M.; Hayward, P. J. *J. Chem. Soc. A* **1970**, 1352.
(47) Dowsing, R. D.; Gibson, J. F. *J. Chem. Phys.* **1969**, *50*, 294.
(48) Sweeney, W. V.; Coucouvanis, D.; Coffman, R. F. *J. Chem. Phys.* **1973**, *59*, 369.
(49) Mathur, P.; Dismukes, G. C. *J. Am. Chem. Soc.* **1983**, *105*, 7093.
(50) Hudson, A.; Kennedy, M. J. D. G. *Inorg. Nucl. Chem. Lett.* **1971**, *7*, 333.

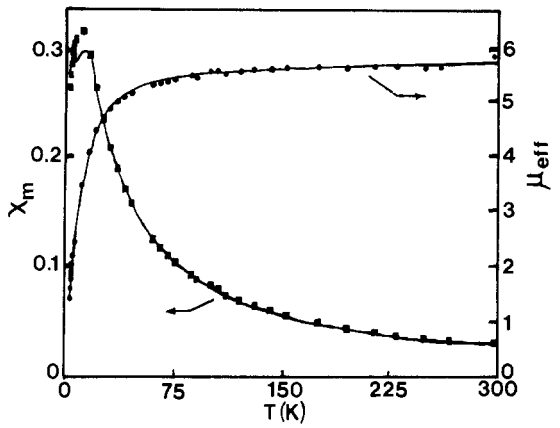

Figure 7. Variation of χ_M and μ_{eff} with temperature for a powder sample of $[Mn(SALPS)]_2$. The data were fitted to the Van Vleck equation[20] for a dimeric spin $^5/_2$–$^5/_2$ system. The fits to both parameters are illustrated as solid lines.

when two $S = {}^5/_2$ ions are coupled, a system with 36 spin states is generated. These states are grouped into 6 manifolds with S = 0, 1, 2, 3, 4, and 5. Ninety $\Delta M_s = 1$ transitions are possible since each manifold has degeneracy equal to $2S + 1$ (with the possibility of each having different zero-field splitting parameters) which can be oriented along each magnetic field axis. Furthermore, $\Delta M_s \neq 1$ transitions are possible. For these reasons, a detailed interpretation of the spectrum has not been attempted. However, a few important features are noteworthy. A literature has been developed[51-55] for antiferromagnetic exchange interactions between binuclear Mn(II) centers doped into divalent oxides and sulfides, and recently these interactions have been interpreted for binuclear Mn(II) Schiff base[42] and semiquinone complexes.[49] First, a comparison of $Mn(SALPS)CH_3OH$ (Figure 6a) and $[Mn(SALPS)]_2$ (Figure 6b) illustrates that there are more fine-structure features more closely spaced for the dimer than for the monomer. This results from the greater number of possible transitions for a binuclear Mn(II) center than for a mononuclear Mn(II) ion.[42] Second, for systems that have weak coupling between identical nuclei, the hyperfine interval is A/n, where A is the observed single nuclei coupling constant and n is the number of coupled nuclei.[52] In this system, the hyperifne interaction can be described by $(a/2)S \cdot I$, where $S = S_i = S_j$ and $I = I_i + I_j$ correspond to atoms i and j with electronic spin S_i and S_j and nuclear spin I_i and I_j, respectively. Thus the A value for $[Mn(SALPS)]_2$ should be half the value for $Mn(SALPS)CH_3OH$. This prediction is observed experimentally in this system (A = 47 G, $[Mn(SALPS)]_2$; A = 93 G, $Mn(SALPS)CH_3OH$). Finally, the number of hyperfine lines for an oriented system is equal to $2[I_i + I_j] + 1$. The spectrum of Figure 6b contains groups of approximately 11 lines. The actual pattern arises from the averaging of signals in the powder. Although the data have not been quantitatively simulated, we believe this spectrum clearly demonstrates that the Mn(II/II) dimer retains its integrity in frozen toluene solution.

For this model to be valid, the exchange coupling constant J must be small. We have collected variable-temperature magnetic data between 1.9 and 300 K, which are illustrated as μ_{eff} or χ_m vs. T in Figure 7. These data were fitted to the theoretical equation for an isotropic magnetic exchange between two spin-$^5/_2$ ions by employing the equation presented by Wojciechowski.[20] The lines in Figure 7 illustrate this fit. The best fitting parameters are $J = -1.88$ (6) cm^{-1} and $g_{av} = 2.00$. There was no evidence for a contribution to χ_m from a small amount of paramagnetic impurity so a correction, as has been described previously,[57] was not employed. The error associated with J may be underestimated since the magnitude of D has not been explicitly determined. Thus, in the region that best defines J (very low T) the zero-field splitting may contribute to the magnetic behavior. Recently, Hendrickson[42] has reported the magnetic properties and EPR spectra for $[Mn(SALDIEN)]_2$. In this example, μ_{eff} = 5.71 at 70 K and 1.85 at 1.7 K with $J = -0.65$ cm^{-1} and $g_{av} = 2.00$. In comparison, μ_{eff} = 5.42 at 70 K and 1.41 at 1.93 K for $[Mn(SALPS)]_2$. These data demonstrate that $[Mn(SALPS)]_2$ has an antiferromagnetic exchange interaction comparable to, but slightly larger than, that of $[Mn(SALDIEN)]_2$. Thus we can conclude that $J = -1.88$ cm^{-1} is consistent with these data and that the weak local coupling assumed for the interpretation of the $[Mn(SALPS)]_2$ EPR spectrum is valid.

Scheme I

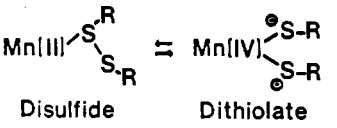

It should be noted that the antiferromagnetic exchange interactions for other manganese(II) systems have been reported. The proposed diphenoxy-bridged dimer $[Mn^{II}SALEN]_2$[37,38] has $J = -6.5$ cm^{-1}. The trigonal-bipyramidal complexes $Mn_2(tren)_2L_2$[15] (where L = NCO^- or NCS^-) form hydrogen-bonded dimers in the solid state with Mn–Mn distances 5.89 and 5.873 Å for the NCO^- and NCS^- species, respectively.[41] The coupling in this case is very small ($J = -0.15$ cm^{-1}). A larger exchange parameter, $J = -18.3$ cm^{-1}, is reported for an Mn(II) ion bridged to two Mn(III) ions by thiolate sulfur atoms (Mn(II)–Mn(III) = 3.11 Å).[13]

Hendrickson and co-workers[42] have supplied strong supporting evidence for the proposal[59] that $[Mn(SALDIEN)]_2$ forms an octahedral diphenoxy-bridged dimer rather than a centrosymmetric dimer[60] similar to $[Cu(SALDIEN)]_2$, which crystal structure analysis shows to have pentacoordinate Cu(II) atoms bound by three atoms from one SALDIEN unit and two atoms from another SALDIEN ligand. This evidence included a comparison of the unit cell parameters for $[Mn(SALDIEN)]_2$ and $[Cu(SALDIEN)]_2$, which were distinctly different, and the similarity of the magnetic behavior of $[Mn(SALDIEN)]_2$ to that of $[Fe(SALDIEN)]_2$ ($J = -2.2$ cm^{-1})[61] and not to that of $[Cu(SALDIEN)]_2$ (no appreciable magnetic interaction between copper atoms).[42]

Our data provide additional support for their structural assignment. The X-ray data unequivocally demonstrate that the Mn(II) ions in $[Mn(SALPS)]_2$ are bridged by two phenolate anions, forming the analogous structure proposed for $[Mn(SALDIEN)]_2$. The antiferromagnetic exchange interactions for $[Mn(SALPS)]_2$ and $[Fe(SALDIEN)]_2$ are nearly identical and are on the same order of magnitude as those of $[Mn(SALDIEN)]_2$. At this juncture, we cannot determine whether the larger J for $[Mn(SALPS)]_2$ relative to that for $[Mn(SALDIEN)]_2$ results from a shorter Mn(II)/Mn(II) distance or from a more effective exchange pathway in the SALPS dimer.

An interesting feature of $[Mn(SALPS)]_2$ and related dimers[42,43,49,50] is the observation of an EPR spectrum. Although both ions are in the +2 oxidation state, a spectrum is seen because the magnetic interaction between centers is small. Thus, these compounds serve as a reminder that the observation of an EPR signal in a dimeric complex is, alone, insufficient evidence for the assignment of the material as a mixed-valence compound. Only when additional information, such as detailed magnetic data, are

(51) Coles, B. A.; Orton, J. W.; Owen, J. *Phys. Rev. Lett.* **1961**, *4*, 116.
(52) Harris, E. A.; Owen, J. *Phys. Rev. Lett.* **1963**, *11*, 9.
(53) Brown, M. R.; Coles, B. A.; Owen, J.; Stevenson, R. W. H. *Phys. Rev. Lett.* **1961**, *7*, 246.
(54) Ishikawa, Y.; *J. Phys. Jpn.* **1966**, *21*, 1473.
(55) Harris, E. A. *J. Phys. C* **1972**, *5*, 338.
(56) Owen, J. *J. Appl. Phys.* **1961**, *32*, 2135.
(57) Apieo, C. L.; Lambert; S. L.; Smith, T. J.; Duesller, E. N.; Gagne, R. R.; Hendrickson, D. N. *Inorg. Chem.* **1981**, *20*, 1229.
(58) Asmussen, R. W.; Soling, H. *Acta Chem. Scand.* **1957**, *11*, 1331.
(59) Zelentsov, V. V.; Somova, I. K.; Kurtanidze, R. Sh.; Korotkova, V. V.; Tsintsadze, G. V. *Koord. Khim.* **1981**, *7*, 1072.
(60) McKenzie, E. D.; Sevley, S. J. *Inorg. Chim. Acta* **1976**, *18*, L1.
(61) Tuchagues, J. P.; Hendrickson, D. N. *Inorg. Chem.* **1983**, *22*, 2545.

in hand can such an assignment be safely made.

An interesting feature of the Mn(SALPS) unit is the Mn(II)–disulfide bond. As shown in Scheme I, an Mn(II)–disulfide lies at one extreme of an internal electron-transfer network. An Mn(IV)–dithiolate can be formulated at the other end of the system. That Mn(SALPS) lies at the extreme left of this diagram is supported by the following observations: (1) the S1–S2 bond length is typical of a coordinated disulfide; (2) while S2 is in bonding distance of the Mn, S1 is nearly 4 Å from the Mn atom; (3) the magnetic data are consistent with a high-spin Mn(II) formulation (μ = 5.94 μ_B). This result is not surprising as Mn(IV) is a strongly oxidizing species and would be expected to undergo redox reactions with thiolate sulfur atoms; however, the notion that the disulfide functional group may act as a two-electron sink for the internal transformation of oxidation states in a given complex represents a fertile area for future studies. In this regard, we are presently investigating the preparation of Mn(I)–disulfides as precursors to Mn(III)–dithiolates.

Acknowledgment. We wish to thank Professor J. L. Dye for the use of the SQUID susceptometer and Joe Skywora and Ira Finkelstein for experimental assistance. We also wish to thank Professors D. Coucouvanis, P. Rasmussen, and A. Francis for enlightening discussions. This work was supported by the donors of the Petroleum Research Fund, administered by the American Chemical Society, and the Horace H. Rackham Foundation.

Supplementary Material Available: Table VII, fractional atomic coordinates for hydrogen atoms of Mn(SALPS)CH_3OH·CH_3OH, Table VIII, thermal parameters for Mn(SALPS)CH_3OH·CH_3OH, Table IX, bond distances for Mn(SALPS)CH_3OH·CH_3OH, Table X, bond angles for Mn(SALPS)CH_3OH·CH_3OH, Table XII, thermal parameters for $[Mn(SALPS)]_2$·$2CH_3CN$, Table XIII, bond distances for $[Mn(SALPS)]_2$·$2CH_3CN$, Table XIV, bond angles for $[Mn(SALPS)]_2$·$2CH_3CN$, Table XVI, χ_m values for $[Mn(SALPS)]_2$, Table XVII, μ_{eff} for $[Mn(SALPS)]_2$, and Table XVIII, fractional atomic coordinates for hydrogen atoms of $[Mn(SALPS)]_2$·$2CH_3CN$, and Figure 8, numbering scheme for Mn(SALPS)CH_3OH·CH_3OH, Figure 9, numbering scheme for $[Mn(SALPS)]_2$·$2CH_3CN$, Figure 10, stereoview of $[Mn(SALPS)]_2$, and Figure 11, packing diagrams for Mn(SALPS)CH_3OH·CH_3OH and $[Mn(SALPS)]_2$·$2CH_3CN$ (19 pages); Table XI, structure factors for Mn(SALPS)CH_3OH·CH_3OH, and Table XV, structure factors for $[Mn(SALPS)]_2$·$2CH_3CN$ (27 pages). Ordering information is given on any current masthead page.

Contribution from the Inorganic Chemistry Laboratory, ETH-Zentrum, CH-8092 Zürich, Switzerland, and Department of Chemistry, Politecnico di Milano, I-20133 Milan, Italy

Preparative and ^{1}H NMR Spectroscopic Studies on Palladium(II) and Platinum(II) Quinoline-8-carbaldehyde (1) Complexes. X-ray Structures of the Cyclometalated Acyl Complex $\overline{PdCl(C(O)C_9H_6N)}(PPh_3)$·$PPh_3$ and *trans*-$PtCl_2(1)(PEt_3)$

A. Albinati,*‡ C. G. Anklin,† F. Ganazzoli,‡ H. Rüegg,† and P. S. Pregosin*†

Received July 22, 1986

A series of complexes of the type *trans*-$PtCl_2$(quinoline-8-carbaldehyde)L (**2**; L = PEt_3, $PTol_3$ (Tol = *p*-$CH_3C_6H_4$), PPh_3, $AsMe_3$, $AsEt_3$, As-*i*-Pr_3, As-*n*-Bu_3, $AsTol_3$, $AsMePh_2$) have been synthesized and characterized. The aldehyde proton couples to ^{195}Pt with a value between 12.4 and 19.7 Hz. We interpret these NMR spectroscopic data as implying a weak Pt←H–C(O) interaction that is not of the previously reported agostic type. Complexes **2** cyclometalate at the aldehyde carbon in refluxing $CHCl_3$. The structure of an intermediate of type **2**, with L = PEt_3, has been determined. Complex **2a** has a square-planar trans geometry with the C–H vector of the aldehyde pointing toward the platinum and the aldehyde oxygen away from the metal center. The molecule is monoclinic, space group $P2_1/c$, with a = 14.411 (3) Å, b = 9.172 (2) Å, c = 15.217 (4) Å, β = 107.07 (2)°, V = 1929.5 Å^3, and Z = 4. The X-ray structure of the palladium acyl complex $\overline{PdCl(C(O)C_9H_6N)}(PPh_3)$·$PPh_3$ (**3**) is reported. The molecule has a square-planar coordination sphere with the acyl carbon trans to Cl and phosphorus trans to the quinoline nitrogen. A molecule of PPh_3 is trapped in the crystal lattice. The molecule crystallizes in the space group $P2_1/c$, with a = 10.159 (4) Å, b = 18.262 (5) Å, c = 21.171 (5) Å, β = 103.27 (3)°, and Z = 4. The long Pd–Cl bond separation of 2.421 (2) Å is in keeping with a large trans influence for the acyl function.

Introduction

Although the cyclometalation of aromatic, and to a lesser extent aliphatic, carbon atoms is widely recognized,[1,2] there is relatively little known concerned with the cyclometalation of aldehyde functions. We have shown that both 2-hydroxy-[3] and 2-(dimethylamino)benzaldehyde[4] can be made to cyclometalate at the aldehyde carbon by using Pd(II) and Pt(II) salts, and Landvatter and Rauchfuss[5] have shown a similar reaction with 2-(diphenylphosphino)benzaldehyde. In all three cases the coordination of either an oxygen, nitrogen, or phosphorus function precedes the cyclometalation. We have recently[6] explored similar chemistry starting from the Pd(II) and Pt(II) dimers $[MCl(\mu\text{-}Cl)l]_2$ plus quinoline-8-carbaldehyde (**1**) (see eq 1). Surprisingly, we have

$$^1/_2[PtCl(\mu\text{-}Cl)(PEt_3)]_2 + \mathbf{1} \rightarrow \mathbf{2} \xrightarrow{\Delta} \overline{PtCl(C(O)C_9H_6N)}(PEt_3) + HCl \quad (1)$$

observed a 13.7-Hz proton–platinum-195 coupling constant (I = $^1/_2$, natural abundance = 34%) between the metal and the aldehyde proton in complex **2a**, an intermediate leading to the acyl complex. The X-ray crystallography for **2a** (see below) clearly shows the C–H vector of the aldehyde to be situated favorably for an interaction with the platinum, so that our solution NMR

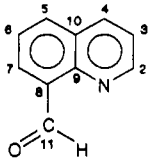

1

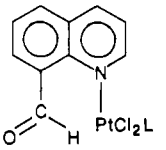

2

L = (a) PEt_3, (b) $PTol_3$, (c) PPh_3, (d) $AsMe_3$, (e) $AsEt_3$, (f) As-*i*-Pr_3, (g) As-*n*-Bu_3, (h) $AsTol_3$, (i) $AsMePh_2$

† ETH-Zentrum.
‡ Politecnico di Milano.

(1) Constable, E. C. *Polyhedron*, **1984**, *3*, 1037.
(2) Bruce, M. I. *Angew. Chem., Int. Ed. Engl.* **1977**, *16*, 73.
(3) Anklin, C.; Pregosin, P. S.; Bachechi, F.; Mura, P.; Zambonelli, L. *J. Organomet. Chem.* **1981**, *222*, 175. Motschi, H.; Pregosin, P. S.; Rüegger, H. *J. Organomet. Chem.* **1980**, *194*, 397.
(4) Anklin, C. G.; Pregosin, P. S. *J. Organomet. Chem.* **1983**, *243*, 101.
(5) Landvatter, E. F.; Rauchfuss, T. B. *Organometallics* **1982**, *193*, 506.
(6) Albinati, A.; Anklin, C. G.; Pregosin, P. S. *Inorg. Chim. Acta* **1984**, *90*, L37.

0020-1669/87/1326-0503$01.50/0 © 1987 American Chemical Society